

Ser
TH1
N21d
no. 1613
c. 2
BLDG

**National Research
Council Canada**

Institute for
Research in
Construction

**Conseil national
de recherches Canada**

Institut de
recherche en
construction

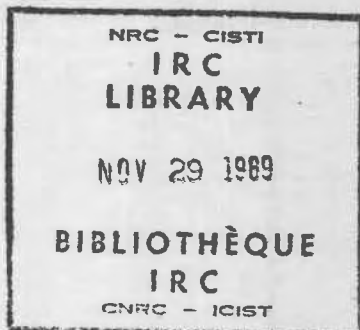
Vapor Transport Characteristics of Mineral Fiber Insulation From Heat Flow Meter Measurements

by M.K. Kumaran

ANALYZED

Reprinted from
Water Vapor Transmission Through Building Materials
and Systems: Mechanisms and Measurement
ASTM, STP, 1039
p. 19-27
(IRC Paper No. 1613)

NRCC 30889



Canada

9242769

CISTI / ICIST



3 1809 00210 7735

Résumé

Deux coefficients empiriques sont identifiés pour représenter la migration de la vapeur d'eau à travers un isolant. Ces coefficients sont déterminés.

Mavinkal K. Kumaran¹

Vapor Transport Characteristics of Mineral Fiber Insulation from Heat Flow Meter Measurements

REFERENCE: Kumaran, M. K., "Vapor Transport Characteristics of Mineral Fiber Insulation from Heat Flow Meter Measurements," *Water Vapor Transmission Through Building Materials and Systems: Mechanisms and Measurement, ASTM STP 1039*, H. R. Trechsel and M. Bomberg, Eds., American Society for Testing and Materials, Philadelphia, 1989, pp. 19-27.

ABSTRACT: Two empirical coefficients are identified to represent water vapor transport through fibrous insulation, in the presence of a thermal gradient. These coefficients are determined from heat flow meter measurements.

KEY WORDS: fibrous insulation, thermal gradient, vapor transport, heat flux, transport characteristics, water vapor transmission, testing

Thermal insulation in a building envelope, like any other component, is subject to gradients in temperature, air pressure, and water vapor pressure. These gradients induce the transport of energy, air, and moisture across the insulation. Traditionally, various transport coefficients are used to represent the transport processes. One such transport coefficient, which is commonly used with reference to water vapor transport, is water vapor permeability, μ , defined as

$$\mu = \frac{W \cdot L}{A \cdot t \cdot \Delta p} \quad (1)$$

where W is the mass of water vapor that flows through the material of thickness, L , across an area of cross-section, A , in time, t , induced by a water vapor pressure difference, Δp . ASTM has prescribed a standard test method, ASTM Test Methods for Water Vapor Transmission of Materials (E 96-80), to determine the water vapor permeability, μ , of different materials.

ASTM E 96-80 is essentially an isothermal method. But a series of recent investigations at the Institute for Research in Construction (IRC) has shown that the influence of thermal gradient, as a driving force, on vapor transport has to be properly accounted for. Therefore, the test methods used to determine moisture transport characteristics should provide information on the relationship between thermal gradient and the transport process. Several experimental and analytical investigations were undertaken at IRC to meet this objective. Some of the information generated has already been reported [1-3]. In particular, an experimental method was identified [1] to determine two moisture transport characteristics

¹ Associate research officer, Institute for Research in Construction, National Research Council, Ottawa, Ontario, Canada K1A 0R6.

of fibrous thermal insulation. The method was subsequently applied [3] to different specimens of glass fiber insulation with densities varying between 15 and 120 kg/m³. The present investigation was undertaken to examine the effect of specimen thickness on the moisture transport characteristics.

Materials and Method

A sample of a medium-density (≈ 45 kg/m³) glass fiber insulation, exposed to laboratory conditions (294 K and 40% relative humidity) for several weeks, with an average thickness of 15 cm was chosen for the experimental investigation. A 57 by 57 cm slab was cut from the sample. This slab was then sliced to give five layers, each with an average thickness of 2.5 cm. Each of these slices was then put in a wooden frame that sealed the edges. The wooden frame was coated with spray paint to reduce moisture migration into the wood. The bulk densities of individual layers of the specimen were 41.3, 41.9, 44.6, 44.9, and 50.8 kg/m³.

As in the previous studies [1-3], the equipment used for the present investigation was a standard 60-cm horizontal heat flow meter (HFM) apparatus, according to ASTM Test Method for Steady-State Heat Flux Measurements and Thermal Transmission Properties by Means of the Heat Flow Meter Apparatus (C 218-71). Heat flowed vertically upwards through the specimen. The simultaneous heat and moisture transport investigated is schematically shown in Fig. 1. In this process, a fixed amount of liquid water, initially present at the hot surface at a temperature, T_H , is transported completely to the cold surface at a temperature, T_C , through the bulk of the insulation. The details of the measurements were reported elsewhere [1].

Measurements were started on a single slice. The slice was laid flat on a platform, and approximately 0.1 kg of water was sprayed on the top surface as uniformly as possible. That specimen was then sealed in a tight-fitting polyethylene bag and placed in the HFM apparatus, the wet surface of the specimen being in contact with the hotter plate of the apparatus. The heat flux through the specimen was then monitored for at least 24 h. This experiment was then repeated for four other pairs of hot and cold surface temperatures according to the sequence outlined in Ref 1. Then the specimen was taken out of the polyethylene bag, and a second slice was placed over it in contact with the dry surface (the hot surface in the latest of the five experiments). Any gap between the wood frames of the two slices was sealed with plastic tape. This combination of two slices provided a second specimen that differed from the first mainly in thickness. The new specimen was then sealed tight in a polyethylene bag as before and another series of five experiments with different pairs of hot and cold surface temperatures was carried out. The whole procedure was repeated with combinations of three, four, and five slices.

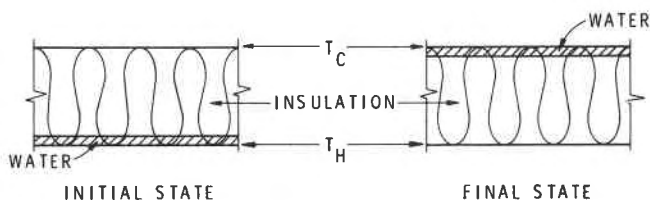


FIG. 1—Schematic representation of the simultaneous heat and moisture transfer investigated; T_H is the hot surface temperature and T_C is the cold surface temperature. The thickness of the water layer is approximately 0.25 mm.

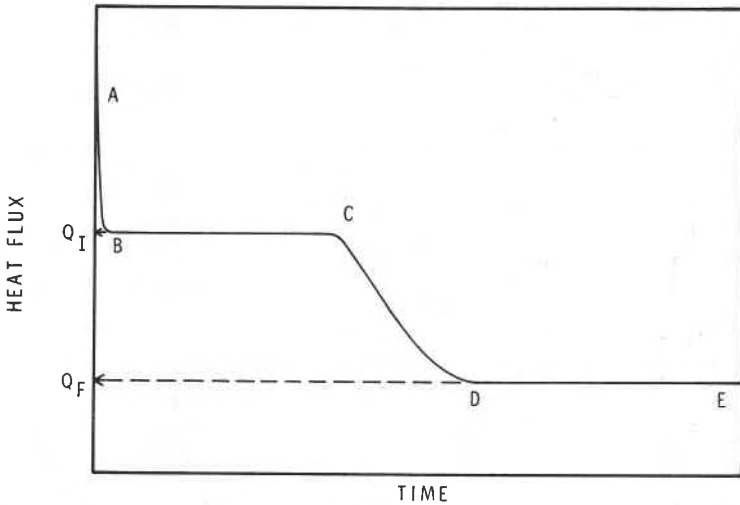
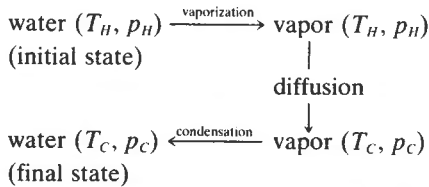


FIG. 2—History of average heat flux during the process represented by Fig. 1; Q_I and Q_F are the heat fluxes during the initial and final steady states.

As in the previous series of investigations [1,2], the history of the heat flux always showed the general behavior represented by Fig. 2. As postulated earlier [1], the initial steady-state (BC) corresponds to a steady, simultaneous transport of heat and moisture, the final steady state (DE) nearly to heat transfer through the dry specimen, and (CD) to a transition between the two steady states. The heat fluxes during the initial and final steady states for all the experiments are given in Table 1. The history of heat flux in the experiments on one slice and five slices are plotted in Fig. 3.

Analysis of the Results and Discussion

The transport of moisture in the process shown in Fig. 1 is the result of the following processes.



As explained in Ref 1, this sequence of processes can be used to calculate the water vapor flux, n , according to the relationship

$$n = (Q_I - Q_F) / (\Delta H_1 + \Delta H_2) \quad (2)$$

where Q_I and Q_F are the mean heat fluxes across the specimen at the initial and final steady states, ΔH_1 is an average specific enthalpy of vaporization in the temperature range T_H to T_C , and ΔH_2 is the specific enthalpy change of water when cooled from T_H to T_C . In Eq 2, Q_I and Q_F are experimental quantities and ΔH_1 and ΔH_2 are available from standard tables

TABLE 1—Experimental results from the heat flow meter measurements; T_H and T_C are the hot and cold surface temperatures, p_H and p_C are the corresponding water vapor pressures, and Q_I and Q_F are the heat fluxes during the initial and final steady states, respectively.

T_H , K	T_C , K	p_H , Pa	p_C , Pa	Q_I , W/m ²	Q_F , W/m ²
ONE SLICE					
307.47	287.34	5 417	1618	69.96	28.00
310.14	287.55	6 275	1640	81.68	31.51
314.67	287.94	7 999	1682	102.53	37.60
320.24	288.42	10 668	1735	131.68	45.36
324.63	288.75	13 280	1772	158.37	51.62
TWO SLICES					
306.49	286.34	5 129	1516	38.06	13.63
310.94	286.48	6 554	1530	49.89	16.71
315.48	286.68	8 347	1550	63.86	19.85
321.34	286.93	11 277	1575	84.81	24.01
326.01	287.32	14 206	1616	103.74	27.34
THREE SLICES					
306.67	286.01	5 181	1483	27.24	9.32
311.11	286.17	6 614	1499	35.92	11.31
315.97	286.34	8 564	1516	47.09	13.59
321.74	286.52	11 505	1534	62.74	16.31
326.53	286.66	14 570	1548	78.72	18.87
FOUR SLICES					
306.53	285.89	5 141	1472	20.97	7.00
311.14	285.98	6 625	1481	28.12	8.59
316.22	286.22	8 677	1504	37.41	10.37
322.16	286.27	11 750	1509	50.78	12.52
326.72	286.39	14 704	1521	62.86	14.17
FIVE SLICES					
306.80	285.94	5 219	1477	17.40	5.66
311.43	285.94	6 730	1477	23.72	6.97
316.32	286.11	8 722	1493	30.73	8.35
322.30	286.34	11 832	1516	42.20	10.05
326.80	286.18	14 761	1500	52.75	11.81

[4]. Thus, the experimental data from Table 1 are used to calculate the moisture fluxes given in Table 2. The differences, $Q_I - Q_F$, observed for each of the five specimens are plotted in Fig. 4 against the corresponding difference, ΔT , in surface temperatures. In Fig. 5, the values of n calculated according to Eq 2 are plotted against ΔT ; and in Fig. 6 against Δp , the difference in saturation water vapor pressure corresponding to ΔT .

The influence of thickness on the magnitude and history of heat flux can be generalized as follows. Figure 3 shows that for a given amount of moisture and a given pair of hot and cold surface temperatures, the thicker the specimen the larger is the duration of the initial steady state. At the same time for a given amount of moisture and for a given thickness, the larger the temperature difference, the shorter is the duration of the initial steady state. Figure 4 shows that for all the five specimens, ΔQ increases with ΔT , but nonlinearly; for a given ΔT , the thinner the specimen, the larger is ΔQ . Figure 5 shows that the influence of the thickness on the water vapor flux is similar to that on ΔQ . But Fig. 6 shows that n is linearly dependent on Δp , the difference in the vapor pressure. However, as summarized in Table 3, a linear least squares analysis of the data from Table 2 shows that n is distinctly non-zero at $\Delta p = 0$. If this residual value is attributed to the coexisting driving force ΔT ,

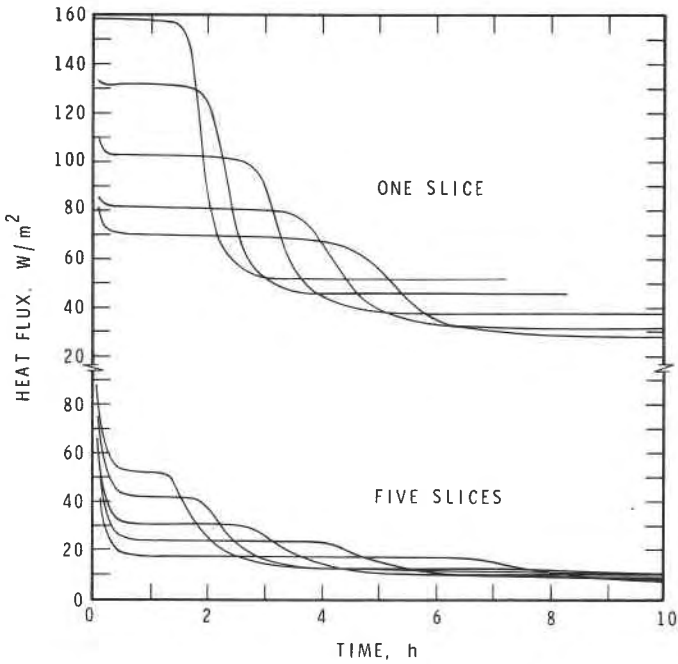


FIG. 3—The history of heat flux from the heat flow meter measurements; the upper group of curves represent one slice and the lower, five slices. In either group, the upper most curve is for the largest difference, ΔT , in surface temperatures (see Table 1) and the successive curves are for decreasing ΔT .

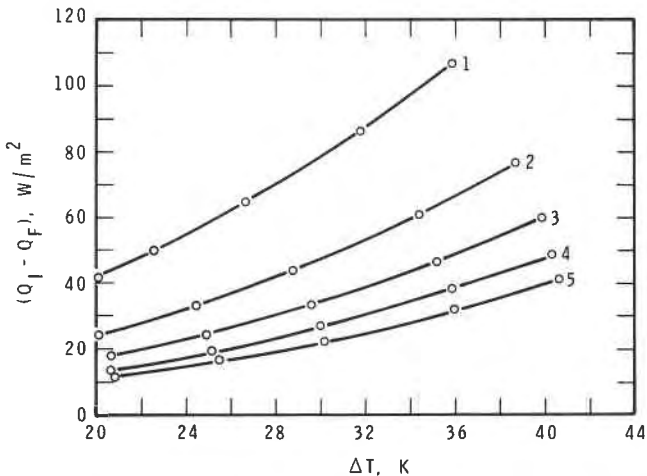


FIG. 4—The dependence of $\Delta Q = Q_1 - Q_F$ on ΔT ; the numbers indicate the number of slices that form the specimen.

TABLE 2—The water vapor flux, n calculated according to Eq 2 from the data in Table 1; $\Delta T = T_H - T_C$ and $\Delta p = p_H - p_C$.

ΔT , K	Δp , Pa	n , mg/(m ² · s)
	ONE SLICE	
20.13	3 799	16.45
22.59	4 635	19.59
26.73	6 317	25.19
31.82	8 933	33.23
35.88	11 508	40.84
	TWO SLICES	
20.15	3 613	9.57
24.46	5 024	12.90
28.80	6 797	17.00
34.41	9 702	23.28
38.69	12 590	29.06
	THREE SLICES	
20.66	3 698	7.01
24.94	5 115	9.56
29.63	7 048	12.92
35.22	9 971	17.74
39.87	13 022	22.71
	FOUR SLICES	
20.64	3 669	5.46
25.16	5 144	7.58
30.00	7 173	10.42
35.89	10 241	14.60
40.33	13 183	18.46
	FIVE SLICES	
20.86	3 742	4.59
25.49	5 253	6.50
30.21	7 229	8.62
35.96	10 316	12.27
40.62	13 261	15.51

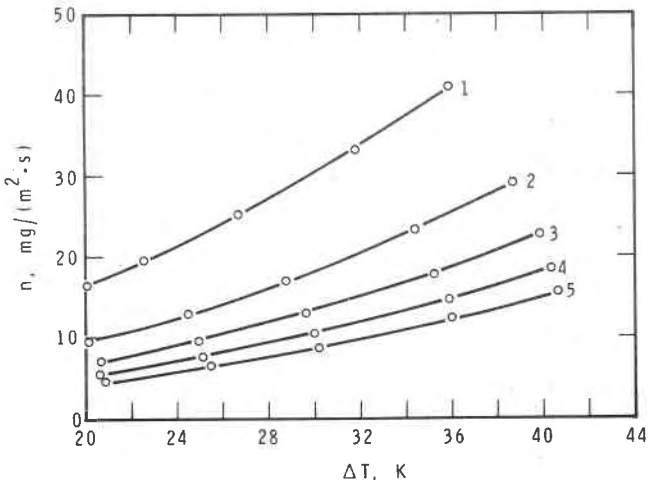


FIG. 5—The dependence of water vapor flux, n , on ΔT ; the numbers indicate the number of slices that form the specimen.

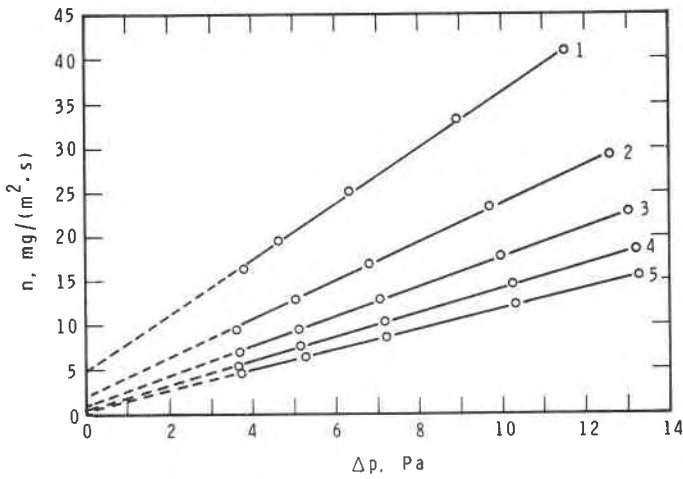


FIG. 6—The linear dependence of water vapor flux, n , on difference Δp in vapor pressure; the numbers indicate the number of slices that form the specimen.

n can be made equal to zero when both ΔT and Δp vanish as

$$n = K_1 \Delta T + K_2 \Delta p \quad (3)$$

Least-squares analyses of the data from Table 2 lead to the values for K_1 and K_2 given in Table 4 and once again confirm that the experimental data on any glass fiber insulation, for the process considered here, can be well represented by the empirical relationship (Eq 3).

The transport coefficients, K_1 and K_2 , in Eq 3 were introduced as characteristics of a specimen. In the present investigation, the five specimens were prepared from the same material. Hence, the data on K_1 and K_2 were used to establish whether or not these coefficients are intensive properties of the material, as follows.

The constants, K_1 and K_2 , for each specimen were multiplied by the corresponding thickness to calculate their values for unit thickness. The values so obtained are plotted in Figs. 7 and 8 against thickness. It is seen that these values depend on the thickness and hence cannot be used as intensive properties for the material. However, the figures show that the relationship between thickness and the empirical constants is not a complex one.

TABLE 3—Results of linear least-squares analysis of the data on n and Δp from Table 2; m is the slope, c is the intercept, and R is the linear correlation coefficient.

Number of Slices	K_1 , $\mu\text{g}/(\text{m}^2 \cdot \text{s} \cdot \text{Pa})$	K_2 , $\mu\text{g}/(\text{m}^2 \cdot \text{s} \cdot \text{K})$	R
One	2.38 ± 0.04	380 ± 10	0.9999
Two	1.87 ± 0.04	150 ± 10	0.9998
Three	1.54 ± 0.02	67 ± 5	0.9999
Four	1.28 ± 0.02	39 ± 4	0.9999
Five	1.09 ± 0.02	28 ± 6	0.9997

TABLE 4—The results of a least-squares analysis of the data from Table 2 according to Eq 3; R is the overall correlation coefficient.

Number of Slices	K_1 , $\mu\text{g}/(\text{m}^2 \cdot \text{s} \cdot \text{Pa})$	K_2 , $\mu\text{g}/(\text{m}^2 \cdot \text{s} \cdot \text{K})$	R
One	2.38 ± 0.04	380 ± 10	0.9999
Two	1.87 ± 0.04	150 ± 10	0.9998
Three	1.54 ± 0.02	67 ± 5	0.9999
Four	1.28 ± 0.02	39 ± 4	0.9999
Five	1.09 ± 0.02	28 ± 6	0.9997

Conclusion

The experimental investigations confirm that the transport of water vapor through any specimen of glass fiber insulation, in the presence of a thermal gradient, can be well represented by two transport characteristics. These transport characteristics can be determined from heat flow meter measurements. The characteristics so determined may not be considered as material properties because they depend on the thickness of the specimen. However, a detailed mathematical analysis of the simultaneous heat and moisture transport represented by Fig. 1 has shown [2] that K_1 and K_2 determined from heat flow meter measurements on a given specimen can be used to calculate the corresponding values for a layer of material of any given thickness within the specimen through a simple linear interpolation.

Acknowledgment

The author gratefully acknowledges the technical assistance of Mr. R. G. Marchand during this investigation.

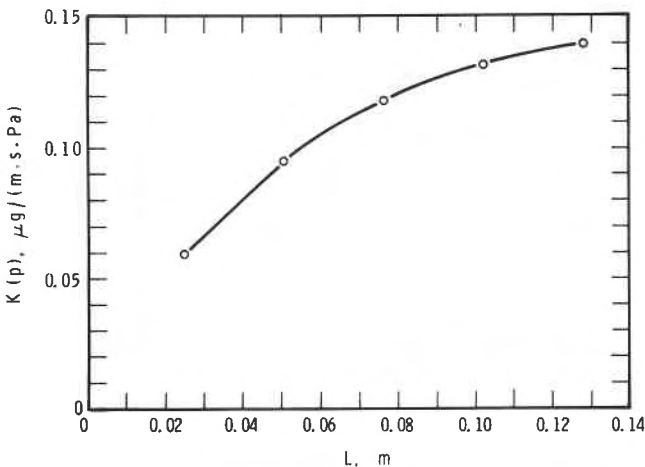


FIG. 7—The dependence of $K(p)$, the value of K_1 for unit thickness on specimen thickness.

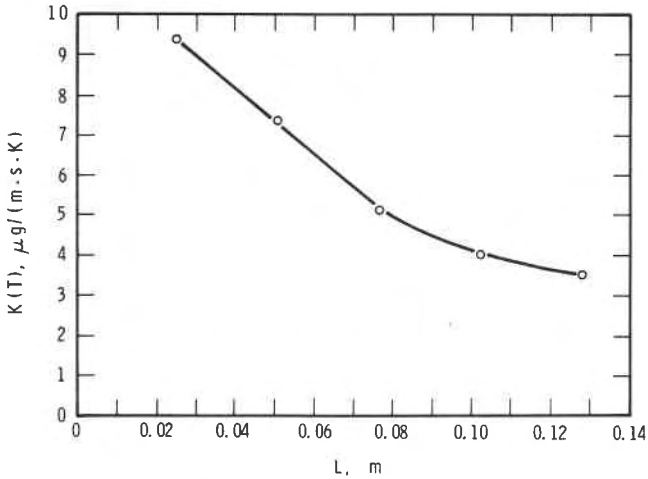


FIG. 8—The dependence of $K(T)$, the value of K_2 for unit thickness on specimen thickness.

References

- [1] Kumaran, M. K., *Journal of Thermal Insulation*, Vol. 10, April 1987, pp. 243–255.
- [2] Kumaran, M. K. and Mitalas, G. P., "Analysis of Simultaneous Heat and Moisture Transport Through Glass Fibre Insulation," *Proceedings, ASME/AIChE National Conference on Heat Transfer*, American Society of Mechanical Engineers/American Institute of Chemical Engineers, HTD—Vol. 78, 1987, pp. 1–6.
- [3] Mitalas, G. P. and Kumaran, M. K., "Simultaneous Heat and Moisture Transport Through Glass Fibre Insulation: An Investigation of the Effect of Hygroscopicity," *Proceedings, ASME Winter Annual Meeting, SED—Vol. 4*, American Society of Mechanical Engineers, 1987, pp. 1–4.
- [4] *ASHRAE Handbook of Fundamentals (SI)*, American Society of Heating, Refrigeration, and Air Conditioning Engineers, 1985, Section 6.5, Table 2.

This paper is being distributed in reprint form by the Institute for Research in Construction. A list of building practice and research publications available from the Institute may be obtained by writing to the Publications Section, Institute for Research in Construction, National Research Council of Canada, Ottawa, Ontario, K1A 0R6.

Ce document est distribué sous forme de tiré-à-part par l'Institut de recherche en construction. On peut obtenir une liste des publications de l'Institut portant sur les techniques ou les recherches en matière de bâtiment en écrivant à la Section des publications, Institut de recherche en construction, Conseil national de recherches du Canada, Ottawa (Ontario), K1A 0R6.